Small-Signal Stability and Dynamic Behaviors of a Hydropower Plant With an Upstream Surge Tank Using Different PID Parameters

GAOHUI LI[1,2], JIAN ZHANG[1], XUMIN WU[2], AND XIAODONG YU[1]

[1]College of Water Conservancy and Hydropower Engineering, Hohai University, Nanjing, Jiangsu 210098, China
[2]POWERCHINA Huadong Engineering Corporation Ltd., Hangzhou, Zhejiang 311122, China

Corresponding author: Xiaodong Yu (yuxiaodong_851@hhu.edu.cn)

ABSTRACT This paper used the state space method to establish a stability analysis model of a hydroturbine governing system (HTGS) coupled with a water diversion system. The stability characteristics of different regulating regions (RRs) were studied according to the eigenvalues of the system, and they were verified by numerical simulations in the time domain. The dynamic system responses and dominating factors were analyzed for governor parameters selected in different domains of the RRs. In addition, an intermediate unstable RR was discovered and its influencing factors were investigated. The results show that the unstable RR occurs because of the interaction between the oscillations in the HTGS and surge tanks and indicate that the system performance varies in different domains of the RR, with better performance observed in domain II. Then, a comprehensive critical stable area is observed in the surge tank based on the effect of the turbine, governor and water inertia, and a specific instance of the traditional Thoma stable area is observed in the proposed area. Either reducing the cross-sectional area of the surge tank and head loss coefficients of the headrace tunnel or increasing the water inertia of the water diversion system can increase the unstable RRs.

INDEX TERMS Hydropower plants, hydroturbine governing system, stability analysis, surge tanks, unstable regulating region.

I. INTRODUCTION

Hydropower is the largest source of renewable electricity generation worldwide and plays a critical role in decarbonizing power systems and improving power system flexibility. With increases in variable renewable sources, such as wind and photovoltaic generation, and the requirement for rapid responses in terms of frequency control, the process of regulating hydropower plants has become more complicated [1], [2]. A hydroturbine governor system (HTGS) is a nonlinear system coupled with hydraulic, mechanical and electrical subsystems. When a small load disturbance signal appears, the governor adjusts the turbine guide vanes according to the signal difference to balance the power system. Fluctuations in system parameters, such as the discharge, surge tank water level, output, and turbine rotational speed, from an initial stable state to another stable state, indicate

that the whole system is under transient process. Moreover, hydropower plants with long headrace or tailrace tunnels are normally equipped with surge tanks to control the water hammer pressure of the spiral case or draft tube. However, as the water level fluctuates over a long period and has a slow decay rate, the stability characteristics of hydropower plants become more complex due to the interaction between the oscillations in the HTGS and surge tanks. If the system design parameters are unreasonable or the tuning of the governor is inappropriate, the oscillations of the system will be unstable during a small load disturbance [3]. The stability and quality of regulation are significant to the safety of the hydropower plant and even to the power system.

A considerable number of studies have been conducted on the regulating stability and quality of HTGSs. Generally, theoretical analysis and numerical simulation are the main tools used to analyze system stability and optimize the regulating quality. A comprehensive summary of the classic mathematical models of an HTGS is presented in [4] and [5],

The associate editor coordinating the review of this manuscript and approving it for publication was Lei Wang.

and some new models and methods are used to describe the characteristics of an HTGS. Xu *et al.* [6] established a Hamilton model of an HTGS and analyzed the dynamic behaviors of the system. Guo *et al.* [7] proposed nonlinear modeling of a hydropower plant with a tailrace tunnel. Yu *et al.* [8], [9] used graph theory to establish the state-space model of an HTGS, and it was then used to solve the complex layout of the water diversion system and connected plants. Eigenvalue methods [10], [11] are commonly used to analyze the stability of an HTGS, and the elasticity of the long penstock can be considered as well [12], [13]. Xu *et al.* [14] summarized different subsystem models and stability analysis approaches for HTGSs along with their applicability in different operational conditions and design layouts. Governor tuning methods are very important for system regulation processes, such as robust control [15], nonlinear generalized predictive control [16], improved particle swarm optimization algorithms [17], and fuzzy sliding mode control [18].

Currently, to ensure the stable operation and regulating quality of an HGTS, the system is often designed to approximate isolated conditions. A large number of islands and remote locations around the world are not serviced by grid power, and hydropower plants in such places are operated under isolated conditions [19], [20]. As a result, the stability of an HTGS with surge tanks is of great concern and a traditional topic of hydropower plant research [21], [22]. Jimenez and Chaudhry [23] provided an analytical criterion for the stability of an isolated hydrounit, including the effects of a water hammer. Chaudhry *et al.* [24] investigated the stability of closed surge tanks with the phase plane method and developed stability criteria. Vereide *et al.* [25] studied the effect of surge tank throttling on system stability and found that the throttle did not have any impact on governor stability. Vournas and Papaioannou [26] analyzed the stability of a hydropower plant with upstream and downstream surge tanks by performing small signal analyses. Guo and Yang [27] presented the critical stable area of the surge tank for primary frequency regulation. Liang *et al.* [28] introduced a novel mathematical model of a Francis hydraulic turbine regulating system with a straight-tube surge tank based on several state-space equations to study the dynamic behaviors of the HTRS system. Liu and Guo [29] investigated the multifrequency dynamic performance of hydropower plants (HPPs) under the coupling effect of a power grid and turbine regulating system with a surge tank.

Previous studies have provided significant insights into the stability of HTGSs with surge tanks. However, the simplified theoretical analysis did not consider the governor effect while the numerical simulation focused on control method optimization. Currently, the Thoma stable area is still used as a surge tank design criterion; however, it neglects many factors, such as the water inertia of the penstock and the effect of the governor. These factors make the stability of the whole system more complex; moreover, the stability characteristics of the entire regulating regions considering the interaction between the oscillations in the HTGS and surge tanks are

unclear. The intermediate unstable regulating region in this study has not ever been mentioned, and significant knowledge gaps remain with respect to its characteristics and influencing factors. The proposed research attempted to address some of these gaps, which are valuable for engineers to design and optimize HTGSs.

This research had two main objectives. The first was to illustrate the stability characteristics of different regulating regions and the corresponding system dynamic behaviors to facilitate the preferred regulating region for the design and operation of hydropower plants. The second objective was to determine the factors that influence the intermediate unstable regulating region. In particular, the effect of the surge tank area was investigated in detail to explore the relationship among the intermediate unstable regulating region, the critical surge tank area proposed in this work and the classical Thoma stable area. In this study, the hydroturbine governing system and mathematical models of its components are briefly introduced and the characteristics of the unstable regulating region and the dynamic behaviors of the HTGS are investigated based on a theoretical analysis and numerical simulation. Then, the effects of the system parameters on the stability are described. Finally, the conclusions are presented and future works are proposed.

II. MATHEMATICAL MODEL

The general layout of the water diversion system with an upstream surge tank in a hydropower plant is shown in Figure 1(a), and a block diagram of the hydroturbine governing system is shown in Figure 1(b).

A. THEORETICAL ANALYSIS MODEL

In this section, the equations used for modeling different parts of the HGTS and water diversion system are introduced. This study focuses on the stability of the ultralow frequency oscillation, which is caused by water level oscillations in the surge tank. The elastic water column has a small effect; therefore, the pipe model used in the theoretical analysis model is based on a rigid water column.

The unsteady flow equation of the headrace tunnel can be given as follows:

$$T_{w1} \frac{\mathrm{d}q_1}{\mathrm{d}t} = -2\alpha_1 \frac{Q_0^2}{H_0} q_1 - Z_u \tag{1}$$

where T_{w1} is the water inertia constant of a headrace tunnel; α_1 is the head loss coefficient of a headrace tunnel; $q_1 = (Q_1 - Q_0)/Q_0$ is the relative value of discharge in a headrace tunnel; Q_1 is the discharge in a headrace tunnel; Q_0 is the initial steady discharge; H_0 is the initial steady operation head of a turbine; $Z_u = (Z - Z_0)/Z_0$ is the relative value of the water level in a surge tank; Z_0 is the initial water level in a surge tank; and t indicates time.

The unsteady flow equation for the penstock is written as follows:

$$T_{w2} \frac{\mathrm{d}q_2}{\mathrm{d}t} = -S_6 \varphi - S_7 \mu - (S_5 + 2\alpha_2 \frac{Q_0^2}{H_0})q_2 + Z_u \tag{2}$$
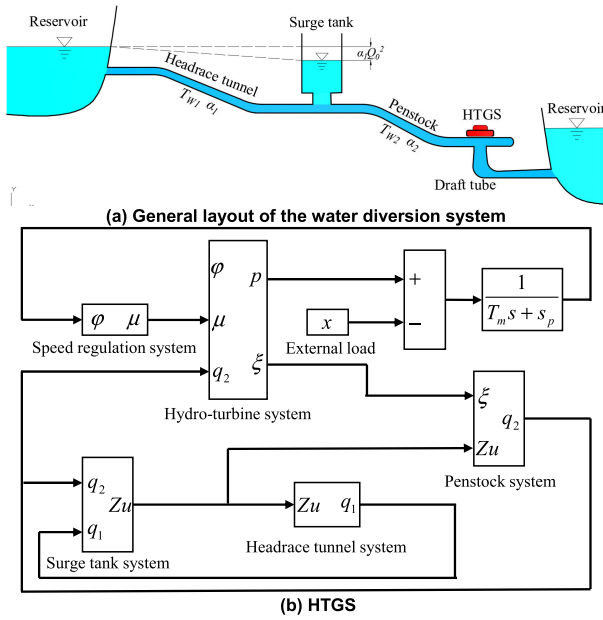
FIGURE 1. Schematic diagram of the HTGS and water diversion system (a) and (b) general layout of the HTGS.

where T_{w2} is the water inertia constant of a penstock; α_2 is the head loss coefficient of a penstock; $q_2 = Q_2 - Q_0/Q_0$ is the relative value of discharge in a penstock; Q_2 is the discharge in the penstock; $S_5 = 2/(1 - S_1)$; $S_6 = -2S_1/(1 - S_1)$; $S_7 = -2S_2/(1 - S_1)$; and S_1 and S_2 are the coefficients of a turbine and reflect the turbine characteristic curves and initial unit operation states [9].

The equation of the surge tank is as follows:

$$F_u \frac{dZ_u}{dt} = \frac{Q_0}{H_0}q_1 - \frac{Q_0}{H_0}q_2 \qquad (3)$$

where F_u is the area of the surge tank.

The frequency equation of the turbine-generator couple is as follows:

$$\frac{d\varphi}{dt} = \frac{S_9 - S_p}{T_m}\varphi + \frac{S_{10}}{T_m}\mu + \frac{S_8}{T_m}q_2 - \frac{1}{T_m}x \qquad (4)$$

where T_m is the mechanical starting time; S_p is the unit self-regulation coefficient; $x = (X - X_0)/X_0$ is the relative value of the external load; X is the external load; X_0 is the initial external load; $S_8 = (1 - S_3/2)S_5$; $S_9 = (1 - S_3/2)S_6 + 1 + S_3$; $S_{10} = (1 - S_3/2)S_7 + S_4$; S_3 and S_4 are the coefficients of a hydroturbine; $\varphi = (n - n_0)/n_0$ is the relative value of the turbine rotating speed; n is the turbine rotating speed; n_0 is the initial steady turbine speed; $\mu = (\tau - \tau_0)/\tau_0$ is the relative value of the guide vane open degree; τ is the guide vane open degree; and τ_0 is the initial steady guide vane open degree.

The equation of the proportion integration differentiation (PID) governor is given as follows:

$$(b_t + b_p)T_d \frac{d\mu}{dt} + b_p\mu = -T_d T_n \frac{d^2\varphi}{dt^2} - (T_n + T_d)\frac{d\varphi}{dt} - \varphi \qquad (5)$$

in which b_t, b_p, T_d, and T_n are the temporary speed drop, permanent speed drop, time constant of the damping device, and prompt time constant, respectively.

The state matrix of the small fluctuations of the system shown in Figure 1 (b) can be obtained using Equations (1) to (5), and the stability can be checked by the eigenvalues of the state matrix [8].

B. TRANSIENT NUMERICAL MODEL

The equations describing the compressible water flow in a pressurized pipeline are as follows:

$$\frac{\partial H}{\partial t} + \frac{a^2}{g}\frac{\partial V}{\partial l} = 0 \qquad (6)$$

$$\frac{\partial H}{\partial l} + \frac{1}{g}\frac{\partial V}{\partial t} + \frac{f|V|V}{2gD} = 0 \qquad (7)$$

where H is the piezometric head; a is the wave speed of the water hammer; V is the flow velocity; g is the acceleration of gravity; l is the distance along the axis of the pipeline; D is the diameter of the pipe; and f is the friction factor of the head loss.

Equations (6) and (7) can be simplified into hyperbolic partial differential equations, which can be solved by the method of characteristics (MOC) [30], [31]. The turbine boundary is obtained from the turbine characteristic curves [32], and the PID governor equation is the same as Equation (5). In addition, other boundary conditions, such as reservoirs, surge tanks, etc., and the solving procedure are provided in [30].

This paper focused on the characteristics of the regulating regions and the dynamic behaviors of a hydropower plant; therefore, some basic mathematical models were only briefly introduced due to space limitations. The detailed models and solution methods can be found in our previous paper [8].

C. HTGS AND WATER DIVERSION SYSTEM DATA

Schematic diagrams of a typical HTGS and a water diversion system of a hydropower plant are shown in Figure 1 (a) and (b). The parameters of the system based on a practical project in China are as follows: the length L_1 and diameter D_1 of the headrace tunnel are 479.95 m and 11.79 m, respectively; the water inertia constant of the headrace tunnel T_{w1} is 3.26 s; the head loss coefficient of the headrace tunnel α_1 is 7.43×10.6 s^2/m^5; the length L_2 and diameter D_2 of the penstock are 309.36 m and 11.14 m, respectively; the water inertia constant of the penstock T_{w2} is 2.35 s; the head loss coefficient of the penstock α_2 is 1.42×10.6 s^2/m^5; the area of surge tank F_u is 1003 m^2; the promptitude time constant T_n is 1.0 s; the permanent speed drop of the governor b_p is 0; the self-regulation coefficient of unit S_p is 0; and other parameters are shown in Table 1. The S subscript indicates the coefficient of the turbine in the table.

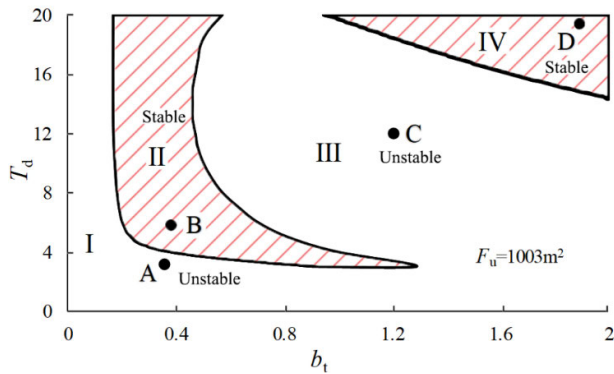|	
Rated output/MW	260.2
Rated discharge (m³/s)	547.91
Rated head	62.97
Rated speed	93.8
Moment of inertia	105700
S_1	-0.091
S_2	0.755
S_3	-1.086
S_4	0.531

FIGURE 2. RRs of the system during a small fluctuation.

III. RESULTS AND DISCUSSION

A. REGULATING REGIONS AND DYNAMIC RESPONSE OF THE SYSTEM

Using Equations (1) to (5), the fifth-order state matrix of the integrated water diversion and power generating system under isolated operating conditions can be obtained and used to describe the stability characteristics of the HTGS. The theoretical model includes the influence of water inertia in the headrace tunnel and penstock, the water level fluctuations in the surge tanks and the characteristics of hydroturbines and governors. Eigenvalues of the state matrix can be solved with QR transformations, and the small fluctuation stability of the system depends on the real part of all eigenvalues, i.e., if all the real parts are negative, then the system is stable; otherwise, it is unstable. By solving all of the eigenvalues corresponding to the different parameters of the governor, the regulating regions (RRs) can be drawn, as shown in Figure 2.

Figure 2 shows that the RRs are separated into two main parts: stable regions (II and IV) and unstable regions (I and III). Due to the intermediate unstable region III between the two stable regions, the system will become unstable when the parameters of the governor increase. However, the stability of the traditional HTGS without considering the effect of the water level fluctuation in the surge tank usually improves with the increment of the parameters of the governor. To determine the origin of unstable region III and verify the theoretical analysis model, the dynamic processes of the system are simulated with two models. The first is the complex transient model based on the water hammer theory and the MOC, and the other is the state-space model based on the rigid water column and fourth-order Runge-Kutta method. If the disturbance is small, then the results of these two models should be consistent. The disturbance to the system is 1% of the rated output, and four groups of governor parameters b_t and T_d are selected randomly in different regions. The variations in the rotating speed of the turbine are shown in Figure 3.

As illustrated in Figure 3, if we choose the parameters of the governor in the stable regions, then the regulating process is convergent; in contrast, if we choose the parameters of the governor in the unstable regions, then the regulating process is diverging. It should be mentioned that the effect of the throttle orifice on the water level fluctuation is neglected due to the linearization in the state-space model; therefore, the bias between the amplitudes of fluctuation in diverging cases increases while the fluctuation period is almost equivalent. Therefore, both models have the same stability characteristics and the results are consistent, which demonstrates that the theoretical analysis model is correct.

Additionally, the dynamic processes of the system vary in different RRs. When the parameters of the governor are selected in region I, the system diverges rapidly and the oscillation period is much shorter than the water level fluctuation period in the surge tank, which is primarily because the parameters of the governor are too small, thereby leading to rapid governor adjustments. Under the water inertia effect of the penstock, the HTGS diverges. When the parameters of the governor are selected in region II, the HTGS and water diversion system are both stable. Additionally, the regulating quality is satisfied with rapid fluctuation damping. Therefore, the parameters of the governor are usually recommended in region II.

When the parameters of the governor are selected in region III, the system diverges, with the divergence period consistent with the fluctuation period of the surge tank, which demonstrates that the water level fluctuation in the surge tank becomes unstable. In this case, the adjustment of the guide vanes slows down as the parameters of the governor increase, thus leading to the extension of the fluctuation period of the HTGS. The water level fluctuation becomes unstable under the effect of the governor. Nevertheless, when the parameters of the governor continue increasing, the adjustment of the guide vanes further decelerate. The adverse impact on the surge tank fluctuation is then reduced, which leads the system to become stable again. An extreme example of this situation is the opening control process, in which the guide vanes remain constant during the load variation, which is absolutely
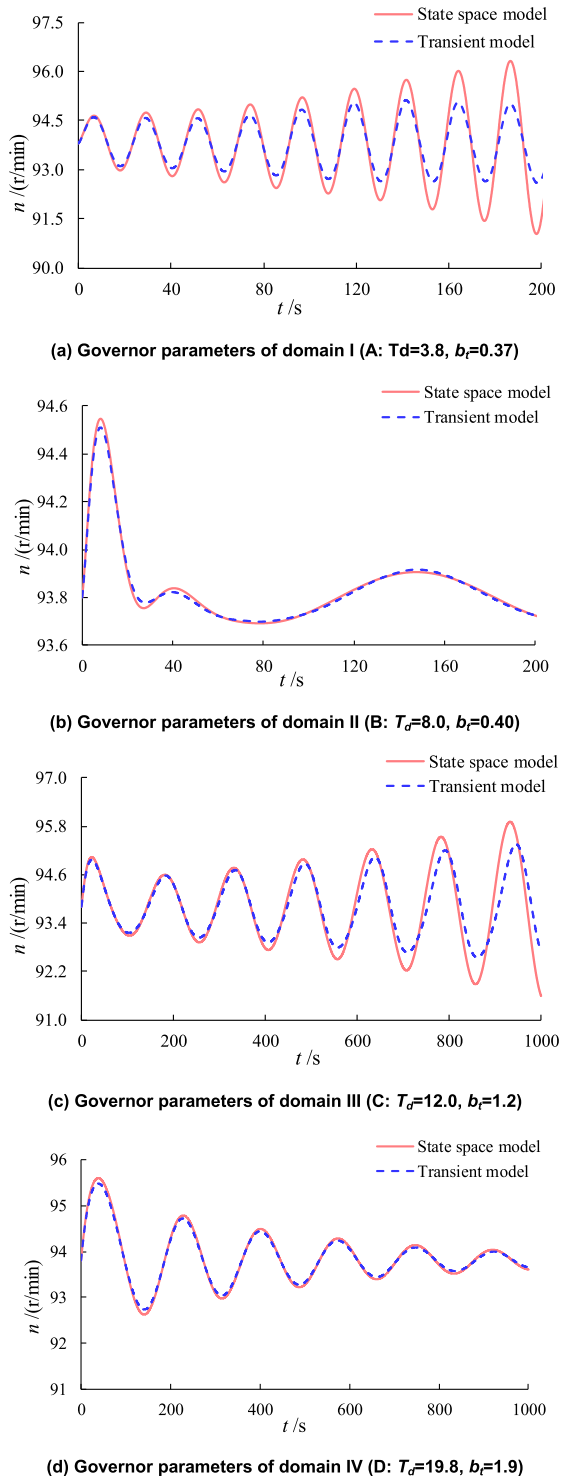
(a) Governor parameters of domain I (A: T_d=3.8, b_t=0.37)

(b) Governor parameters of domain II (B: T_d=8.0, b_t=0.40)

(c) Governor parameters of domain III (C: T_d=12.0, b_t=1.2)

(d) Governor parameters of domain IV (D: T_d=19.8, b_t=1.9)

FIGURE 3. Dynamic process of the system in different regions.

stable [3]. The parameters of the governor in region IV can make the system stable, although the regulating quality is poor in areas where the amplitude of fluctuations is large and the damping is slow.

The regulating regions for the HTGS with surge tanks have an intermediate unstable region. If the parameters of the governor are selected in this region, then the fluctuation of the

system during a small load disturbance will diverge. To determine the influencing factors of the intermediate unstable region, a sensitivity analysis was conducted as described in the next section.

B. SENSITIVITY ANALYSIS OF THE INTERMEDIATE UNSTABLE REGION

In this section, the influences of the cross-sectional area of the surge tank and the water inertia constant and head loss coefficient of the water diversion system on the intermediate unstable region are investigated. The Thoma critical surge tank area [3] is given as follows:

$$F_T = \frac{L_1 F}{2\alpha_1 g(h_0 - h_{f1} - 3h_{f2})} \qquad (8)$$

where F, L_1 and h_{f1} are the cross-sectional area, length and head loss of the headrace tunnel, respectively; α_1 is the head loss coefficient of the headrace tunnel and corresponds to the equation $h_{f1} = \alpha_1 V_1^2$ (V_1 is the velocity of the headrace tunnel); and h_0 and h_{f2} are the stable operating head of the turbine and the head loss of the penstock, respectively. The water inertia constant is defined as $T_w = LV/gh_0$. Equation (8) is widely used to design the surge tank area.

1) INFLUENCE OF THE CROSS-SECTIONAL AREA OF THE SURGE TANK

As indicated in Figure 4, the area of the surge tank has a great impact on the system stability. When the cross-sectional area of the surge tank is smaller than a critical value, an intermediate unstable region is not observed and the lower boundary of the stable region moves toward the bottom left as the surge tank area decreases (as shown in Figure 4(a)). However, although the system can be stable when governor parameters with large values are selected, the regulating quality is poor; in such a case, the dynamic process is similar to the results of region IV in Figure 2.

Figure 4 (b) and Figure 2 show that when the area of the surge tank is approximately 900 m^2, the intermediate unstable region appears, and with increases in the surge tank area, unstable region III decreases. If the surge tank area is large enough, then the unstable region disappears and the role of the surge tank becomes similar to that of a reservoir. In addition, the lower boundary of region II basically does not change, indicating that unstable region I is not affected by the surge tank area. As discussed before, region I is prominently controlled by the HTGS and the water inertia of the penstock. In contrast, when the surge tank area decreases gradually, the upper boundary of region II moves to the lower boundary. When the two boundaries overlap, stable region II disappears, as shown in Figure 4(a).

Therefore, a critical surge tank area occurs that leads to differences in the characteristics of the system stability. If the surge tank area is larger than this critical value, then the stability of the system improves as the surge tank area increases; however, if the surge tank area is smaller than this critical value, then the stability of the system decreases
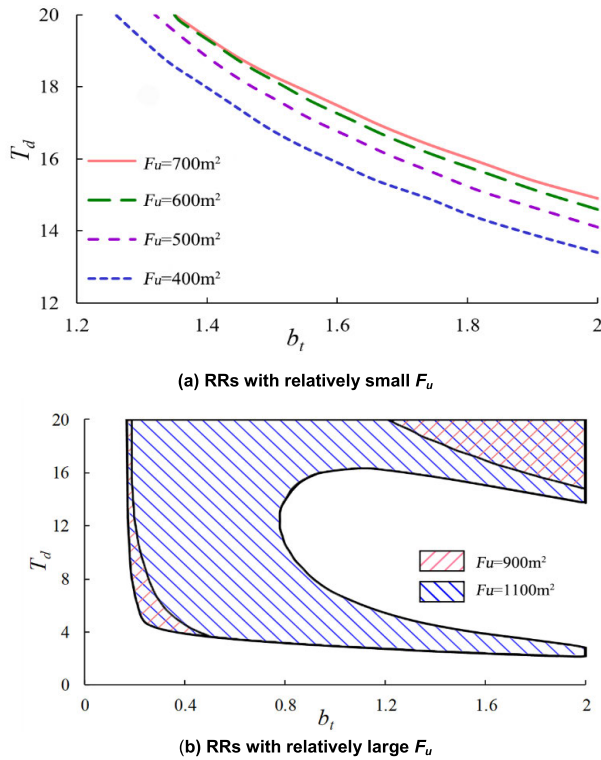
(a) RRs with relatively small F_u

(b) RRs with relatively large F_u

FIGURE 4. RRs of the different cross-sectional areas of the surge.

slightly as the surge tank area increases. As shown in Figure 4, when stable region II disappears or intermediate unstable region III reaches its maximum value, the cross-sectional area becomes the critical surge tank area considering the effect of the hydroturbine characteristics, water inertia, governor characteristics, etc. When the surge tank area is defined as F_u and the critical surge tank area is F_c, if F_u is greater than F_c, then stable region II appears, in which both the stability and regulating quality are better. If F_u is smaller than F_c, then stable region II disappears, and only the unstable region and stable region IV remain. Even if the system is stable in region IV, the regulating quality is poor and the requirements will not be met.

As shown in Table 1, the Thoma critical surge tank area F_T of the system is 498 m^2 according to Equation (8) while the critical surge tank area F_c proposed in this study is approximately 900 m^2. However, as shown in Figure 4, if the surge tank area is set to F_T, then the stability of the system will be poor. To analyze the relationship between F_T and F_c, a fourth-order stability analysis model that ignores water inertia in penstocks is established in this section, and the other parameters shown in Table 1 remain consistent. The RRs are shown in Figure 5.

Compared with the RRs in Figure 4, the RRs are greatly changed when the water inertia in the penstock is ignored. A new stable region II appears in the bottom left, even when the surge tank is reduced to 500 m^2 (near F_T); additionally, unstable region I disappears, which means that the governor can regulate rapidly without considering the stability limit of
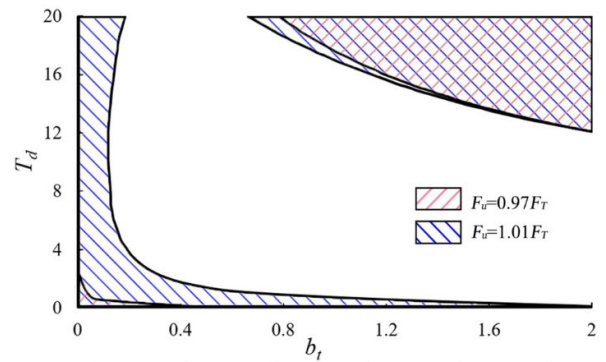
the HTGS. The stability of the water level fluctuation in the surge tank is dominant, and an intermediate unstable region is also observed. According to the definition of the critical surge tank in this study, F_c is reduced to 485 m^2 when the water inertia in the penstock is not considered, and it is slightly smaller than F_T due to the effect of the governor. Thus, the results are consistent with the new definition of the critical surge tank area F_c proposed in this study, and the Thoma area F_T is a specific case that does not consider the water inertia in the penstock and the effect of the governor.

In addition, a comparison of Figure 4 (b) with Figure 5 shows that the critical surge tank area that considers the water inertia in the penstock is almost twice as large as that without considering such inertial. Therefore, the water inertia in the penstock has a great influence on the system stability and the traditional Thoma criterion cannot be used to check the system stability during a small fluctuation, especially for low head hydropower plants with a long penstock.

2) INFLUENCE OF THE PARAMETERS OF THE WATER DIVERSION SYSTEM
a: WATER INERTIA CONSTANT OF THE HEADRACE TUNNEL
First, three different water inertia constants of the headrace tunnel, namely, 0.9 T_{w1}, T_{w1} and 1.1 T_{w1}, were used to analyze the influence of this tunnel on the intermediate unstable region, while the remaining parameters were kept the same. The results for 0.9 T_{w1} and 1.1 T_{w1} are shown in Figure 6, and the result for T_{w1} is shown in Figure 2. Figure 6 indicates that increasing the water inertia constant of the headrace tunnel will enlarge the intermediate unstable region, which deteriorates the stability of the system. Additionally, the water inertia constant of the headrace tunnel only affects the intermediate unstable region, which is related to the stability of the surge tank. However, unstable region I presents limited variations because it depends on the HTGS and the penstock.

b: WATER INERTIA CONSTANT IN THE PENSTOCK
Then, three water inertia constants in the penstock 0.9 T_{w2}, T_{w2} and 1.1 T_{w2} was used to obtain the RRs, and the other parameters were kept the same. The results of T_{w2} are shown in Figure 2, while the others are shown in Figure 7. The
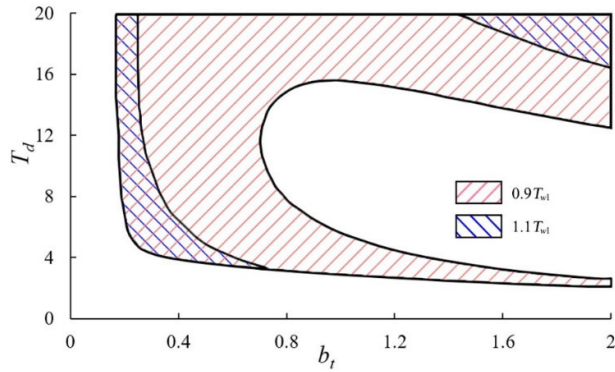
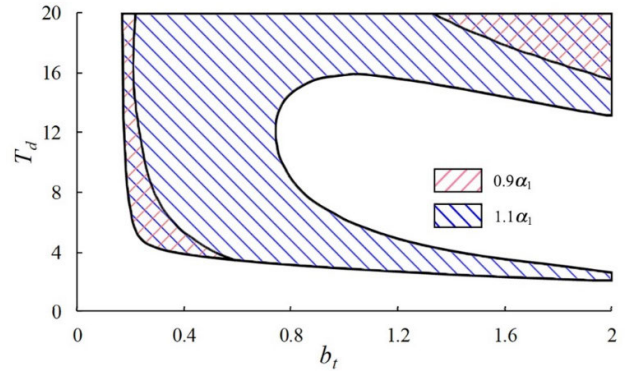**FIGURE 6.** RRs of different water inertia constants of the headrace tunnel.

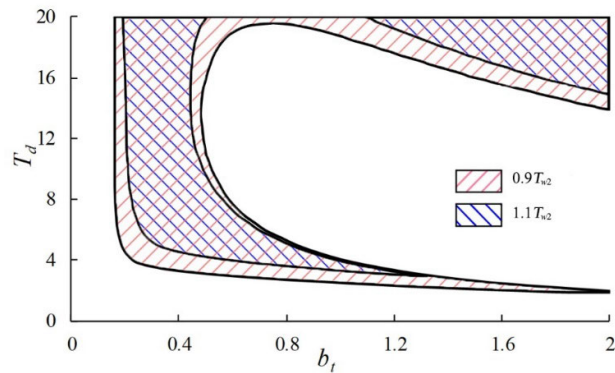**FIGURE 8.** RRs of different head loss coefficients of the headrace tunnel.

FIGURE 7. RRs of different water inertia constants of the penstock.
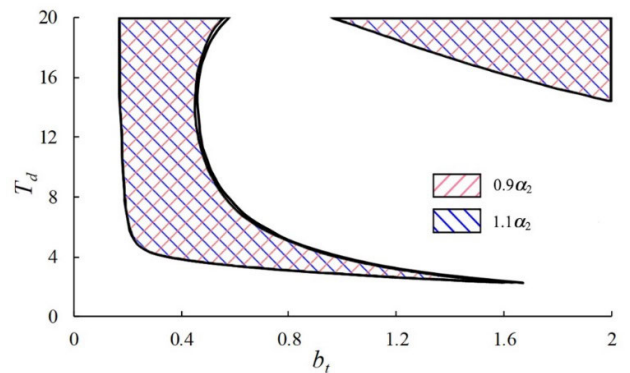

FIGURE 9. RRs of different head loss coefficients of the penstock.

results show that the intermediate unstable region increases with increasing water inertia in the penstock, which adversely affects the system stability. The effect of the water inertia in the penstock is not as sensitive as that in the headrace tunnel. In addition, when the water inertia in the penstock increases, unstable region I enlarges, which is consistent with the previous analysis that the water inertia in the penstock affects the stability of HTGS. If the water inertia is ignored, unstable region I will disappear.

c: HEAD LOSS COEFFICIENT OF THE HEADRACE TUNNEL
Three head loss coefficients of the headrace tunnel, namely, $0.9\,\alpha_1$, α_1 and $1.1\,\alpha_1$, were used to obtain the system RRs. Figure 2 shows the stable region of α_1, and the other results are shown in Figure 8. The results indicate that a large head loss coefficient of the headrace tunnel results in an obvious decrease in the intermediate unstable region, which is similar to the influence of water inertia in the headrace tunnel. Head loss is the origin of the attenuation of the surge tank fluctuation; therefore, the larger the head loss coefficient of the headrace tunnel, the smaller the critical surge tank area. Meanwhile, increasing the head loss coefficient definitely reduces the power output of the hydropower plant.

d: HEAD LOSS COEFFICIENT OF THE PENSTOCK
Finally, three head loss coefficients of the penstock, namely, $0.9\,\alpha_2$, α_2, and $1.1\,\alpha_2$, were utilized to find the system

RRs. The results of α_2 are shown in Figure 2, and the others are shown in Figure 9. The intermediate unstable region is almost the same, which indicates that the head loss coefficient of the penstock has little impact on the system stability and the critical surge tank area.

IV. CONCLUSION
In this study, a theoretical model for analyzing the stability of an HTGS with a water diversion system was established and the eigenvalue method was employed to investigate the RRs. The numerical model of hydraulic transients in hydropower plants was used to verify the theoretical model, and good consistency was obtained between these two models. Based on the models, the stability characteristics of different RRs and the corresponding system dynamic responses were illustrated. In addition, the effect of the water diversion system parameters on the system stability was determined. The findings of this research can be summarized as follows.

(1) An intermediate unstable region exists in the RRs of the HTGS with a surge tank. Traditionally, an HTGS is more stable when the parameters of the governor are larger. However, due to the effect of the water level fluctuation in the surge tank, the system might be unstable when the parameters of the governor increase. The dynamic response of the system varies in different domains of the RRs, and the dominant influencing factors of each domain are different. Generally,

when the parameters of the governor are set in domain II, the regulating stability and quality are better.

(2) The relationship among the intermediate unstable regulating region, the critical surge tank area proposed in this work and the classical Thoma stable area is determined. When intermediate unstable region III reaches its maximum value, the cross-sectional area of the surge tank is the critical surge tank area considering the effect of hydroturbines, water inertia, governor characteristics, etc., and the Thoma stable area is a specific situation that neglects the water inertia in the penstock.

(3) The water inertia in the penstock has a great influence on the system stability, i.e., the critical surge tank area is almost twice the Thoma area in the case study. Therefore, the classical Thoma criterion is not sufficient to check the system stability during small fluctuations, especially for low head hydropower plans with long penstocks. Either reducing the surge tank area and head loss coefficients of the headrace tunnel or increasing the water inertia of water diversion systems can enlarge the unstable RRs.

As this paper mainly investigated the oscillations caused by interactions between an HTGS and water diversion system, electric subsystems, such as automatic voltage regulators (AVCs) and power system stabilizers (PSSs), are simplified. In addition, a mathematical expression of the new critical surge tank area is still needed, which is more general and convenient for practical use. Our group will continue to address these points in future investigations.

APPENDIX A
NOTATION AND NOMENCLATURE

HTGS	hydroturbine governing system
RRs	regulating regions
HPPs	hydropower plants
MOC	method of characteristics
PID	proportion integration differentiation
$[GD^2]$	moment of inertia of rotating fluid and mechanical parts in the turbine-generator unit, [t·m^2]
a	wave speed of water hammer, [m/s]
b_p	permanent speed drop of the governor, [pu]
b_t	temporary speed drop, [pu]
D	diameter of the pipe, [m]
f	the friction factor of head loss, [pu]
F	the cross-sectional area of headrace tunnel, [m^2]
F_u	the cross-sectional area of the surge tank, [m^2]
g	acceleration of gravity, [m/s^2]
h	initial operation head of turbine, [m]
h_f1, h_f2	head loss of headrace tunnel and penstock, [m]
h_0	initial operation head of turbine, [m]
H	piezometric head, [m]
l	the distance along the axis of pipeline, [m]

L	length of the pipeline, [m]
L_1, L_2	length of the headrace tunnel, [m]
n	rotating speed of the turbine, (rad/s)
n_0	the initial rotation speed of turbine, (rad/s)
P	power of turbine, [kw]
p	relative value of power of turbine, $p = (p - p_0)/p_0$, [pu]
P_G	power absorbed by the generator, [kw]
p_G	the relative value of power absorbed by the generator, $p_G = x + s_p\varphi$, $p_G = (P_G - P_{G0})/P_{G0}$, [pu]
Q_1, Q_2	discharge in the headrace tunnel and penstock, [m^3/s]
s_p	unit self-regulation coefficient, $s_p = \partial P_G/\partial\varphi$, [pu]
S_1, S_2, S_3, S_4	coefficients of hydro-turbine, which reflects turbine characteristic curves and initial unit operation states, [pu]
S_5, S_6, S_7	coefficients, [pu]
S_8, S_9, S_{10}	coefficients, [pu]
T	time, [s]
T_d	dashpot time constant, [s]
T_m	mechanical starting time, $T_m = [GD^2]\,n_0^2/365P_0$, [s]
q_1, q_2	the relative value of discharge variation in the headrace tunnel and penstock, [pu]
T_n	promptitude time constant, [s]
T_w1, T_w2	water inertia constant of the headrace tunnel and penstock, $T_{wi} = L_iV_i/gh_0$, [s]
V	flow velocity, [m/s]
V_1, V_2	velocity in the headrace tunnel and penstock, [m/s]
X	external load, [kw]
x	the relative value of external load, $x = (X - X_0)/X_0$, [pu]
Z	the water level in the surge tank, [m]
Z_0	the initial water level in the surge tank, [m]
Zu	relative value of water level variation in the surge tank, [pu]
α_1, α_2	head loss coefficient of the headrace tunnel and penstock, [s^2/m^5]
μ	relative value of the guide vanes open degree, $\mu = (\tau - \tau_0)/\tau_0$, [pu]
τ	guide vanes open degree, [°]
τ_0	initial guide vanes open degree, [°]
φ	the relative value of the rotating speed of turbine, $\varphi = (n - n_0)/n_0$, [pu]
ξ	the relative value of the operation head of turbine, $\xi = (h - h_0)/h_0$, [pu]

REFERENCES

[1] H. Auer and R. Haas, "On integrating large shares of variable renewables into the electricity system," *Energy*, vol. 115, pp. 1592–1601, Nov. 2016.

[2] L. Hirth and I. Ziegenhagen, "Balancing power and variable renewables: Three links," *Renew. Sustain. Energy Rev.*, vol. 50, pp. 1035–1051, Oct. 2015.

[3] M. H. Chaudhry, *Applied Hydraulic Transients*. New York, NY, USA: Springer, 2014.

[4] W. Group Prime Mover and E. Supply, "Hydraulic turbine and turbine control models for system dynamic studies," *IEEE Trans. Power Syst.*, vol. 7, no. 1, pp. 167–179, Feb. 1992.

[5] H. Fang, L. Chen, N. Dlakavu, and Z. Shen, "Basic modeling and simulation tool for analysis of hydraulic transients in hydroelectric power plants," *IEEE Trans. Energy Convers.*, vol. 23, no. 3, pp. 834–841, Sep. 2008.

[6] B. Xu, F. Wang, D. Chen, and H. Zhang, "Hamiltonian modeling of multi-hydro-turbine governing systems with sharing common penstock and dynamic analyses under shock load," *Energy Convers. Manage.*, vol. 108, pp. 478–487, Jan. 2016.

[7] W. Guo, J. Yang, M. Wang, and X. Lai, "Nonlinear modeling and stability analysis of hydro-turbine governing system with sloping ceiling tailrace tunnel under load disturbance," *Energy Convers. Manage.*, vol. 106, pp. 127–138, Dec. 2015.

[8] X. Yu, J. Zhang, C. Fan, and S. Chen, "Stability analysis of governor-turbine-hydraulic system by state space method and graph theory," *Energy*, vol. 114, pp. 613–622, Nov. 2016.

[9] X. Yu, X. Yang, and J. Zhang, "Stability analysis of hydro-turbine governing system including surge tanks under interconnected operation during small load disturbance," *Renew. Energy*, vol. 133, pp. 1426–1435, Apr. 2019.

[10] W. Yang, P. Norrlund, C. Y. Chung, J. Yang, and U. Lundin, "Eigen-analysis of hydraulic-mechanical-electrical coupling mechanism for small signal stability of hydropower plant," *Renew. Energy*, vol. 115, pp. 1014–1025, Jan. 2018.

[11] X. Liu and C. Liu, "Eigenanalysis of oscillatory instability of a hydropower plant including water conduit dynamics," *IEEE Trans. Power Syst.*, vol. 22, no. 2, pp. 675–681, May 2007.

[12] G. Martínez-Lucas, J. I. Sarasúa, J. Á. Sánchez-Fernández, and J. R. Wilhelmi, "Power-frequency control of hydropower plants with long penstocks in isolated systems with wind generation," *Renew. Energy*, vol. 83, pp. 245–255, Nov. 2015.

[13] J. I. Sarasúa, J. I. Pérez-Díaz, J. R. Wilhelmi, and J. Á. Sánchez-Fernández, "Dynamic response and governor tuning of a long penstock pumped-storage hydropower plant equipped with a pump-turbine and a doubly fed induction generator," *Energy Convers. Manage.*, vol. 106, pp. 151–164, Dec. 2015.

[14] B. Xu, J. Zhang, M. Egusquiza, D. Chen, F. Li, P. Behrens, and E. Egusquiza, "A review of dynamic models and stability analysis for a hydro-turbine governing system," *Renew. Sustain. Energy Rev.*, vol. 144, Jul. 2021, Art. no. 110880.

[15] K. Natarajan, "Robust PID controller design for hydroturbines," *IEEE Trans. Energy Convers.*, vol. 20, no. 3, pp. 661–667, Sep. 2005.

[16] C. Li, Y. Mao, J. Yang, Z. Wang, and Y. Xu, "A nonlinear generalized predictive control for pumped storage unit," *Renew. Energy*, vol. 114, pp. 945–959, Dec. 2017.

[17] H. Fang, L. Chen, and Z. Shen, "Application of an improved PSO algorithm to optimal tuning of PID gains for water turbine governor," *Energy Convers. Manage.*, vol. 52, no. 4, pp. 1763–1770, Apr. 2011.

[18] X. Yuan, Z. Chen, Y. Yuan, and Y. Huang, "Design of fuzzy sliding mode controller for hydraulic turbine regulating system via input state feedback linearization method," *Energy*, vol. 93, pp. 173–187, Dec. 2015.

[19] S. V. Papaefthymiou, V. G. Lakiotis, I. D. Margaris, and S. A. Papathanassiou, "Dynamic analysis of island systems with wind-pumped-storage hybrid power stations," *Renew. Energy*, vol. 74, pp. 544–554, Feb. 2015.

[20] S. Padrón, J. Medina, and A. Rodríguez, "Analysis of a pumped storage system to increase the penetration level of renewable energy in isolated power systems. Gran Canaria: A case study," *Energy*, vol. 36, no. 12, pp. 6753–6762, 2011.

[21] H. Bao, J. Yang, G. Zhao, W. Zeng, Y. Liu, and W. Yang, "Condition of setting surge tanks in hydropower plants—A review," *Renew. Sustain. Energy Rev.*, vol. 81, pp. 2059–2070, Jan. 2018.

[22] W. Guo, J. Yang, and Y. Teng, "Surge wave characteristics for hydropower station with upstream series double surge tanks in load rejection transient," *Renew. Energy*, vol. 108, pp. 488–501, Aug. 2017.

[23] O. F. Jiménez and M. H. Chaudhry, "Stability limits of hydroelectric power plants," *J. Energy Eng.*, vol. 113, no. 2, pp. 50–60, Sep. 1987.

[24] M. H. Chaudhry, M. A. Sabbah, and J. E. Fowler, "Analysis and stability of closed surge tanks," *J. Hydraulic Eng.*, vol. 111, no. 7, pp. 1079–1096, Jul. 1985.

[25] K. Vereide, B. Svingen, T. K. Nielsen, and L. Lia, "The effect of surge tank throttling on governor stability, power control, and hydraulic transients in hydropower plants," *IEEE Trans. Energy Convers.*, vol. 32, no. 1, pp. 91–98, Mar. 2017.

[26] C. D. Vournas and G. Papaioannou, "Modelling and stability of a hydro plant with two surge tanks," *IEEE Trans. Energy Convers.*, vol. 10, no. 2, pp. 368–375, Jun. 1995.

[27] W. Guo and J. Yang, "Stability performance for primary frequency regulation of hydro-turbine governing system with surge tank," *Appl. Math. Model.*, vol. 54, pp. 446–466, Feb. 2018.

[28] J. Liang, X. Yuan, Y. Yuan, Z. Chen, and Y. Li, "Nonlinear dynamic analysis and robust controller design for francis hydraulic turbine regulating system with a straight-tube surge tank," *Mech. Syst. Signal Process.*, vol. 85, pp. 927–946, Feb. 2017.

[29] Y. Liu and W. Guo, "Multi-frequency dynamic performance of hydropower plant under coupling effect of power grid and turbine regulating system with surge tank," *Renew. Energy*, vol. 171, pp. 557–581, Jun. 2021.

[30] E. B. Wylie, V. L. Streeter, and L. S. Suo, *Fluid Transients in Systems*. New York, NY, USA: Prentice-Hall, 1993.

[31] M. S. Ghidaoui, M. Zhao, D. A. McInnis, and D. H. Axworthy, "A review of water hammer theory and practice," *Appl. Mech. Rev.*, vol. 58, no. 1, pp. 49–76, Jan. 2005.

[32] X. Yu, J. Zhang, and D. Miao, "Innovative closure law for pump-turbines and field test verification," *J. Hydraulic Eng.*, vol. 141, no. 3, Mar. 2015, Art. no. 05014010.

GAOHUI LI is currently pursuing the Ph.D. degree with Hohai University. He is currently working as a Senior Engineer with POWERCHINA Huadong Engineering Corporation Ltd. His main research interest includes hydraulic transition process of power station and pump station.

JIAN ZHANG is currently a Professor with the College of Water Conservancy and Hydropower Engineering, Hohai University. His main research interests include hydroelectric power station, pump station hydraulics, hydraulic transition process control and simulation of long-distance water supply systems, pumped storage power station, and new energy utilization.

XUMIN WU is currently working as a Senior Engineer with POWERCHINA Huadong Engineering Corporation Ltd. He is also the President of the Institute of Water Resources and Hydropower. His current research interests include hydraulic transition processes and water supply engineering.

XIAODONG YU is currently a Professor with the College of Water Conservancy and Hydropower Engineering, Hohai University. His main research interests include transient flow theory and engineering application, transient process simulation and stability control of hydropower station, and pumping station systems.

• • •